

**Yurii Bilak,
Fedir Saibert,
Roman Buchuk,
Mariana Rol**

ADAPTIVE HYBRID NUMERICAL MODELING OF WAVE PROCESSES IN MULTILAYER STRUCTURES BASED ON TMM AND FEM METHODS

The object of research in this work is wave processes in multilayer thin films and methods of their numerical modeling using adaptive hybrid models. The research covers multilayer media with gradient distribution of physical parameters, including inhomogeneities.

The problem addressed in this study is the enhancement of the accuracy and efficiency of numerical modeling of wave processes in complex multilayered structures while reducing computational costs. Traditional methods, such as the transfer matrix method or the finite element method, have limitations related to computational complexity, numerical stability, and the ability to account for intricate geometric features.

The essence of the obtained results lies in the development and software implementation of an adaptive hybrid model that combines the transfer matrix method for wave propagation calculations in homogeneous regions and the finite element method for modeling complex geometries. The proposed approach optimizes computational resources by dynamically adjusting the grid resolution according to local variations in the refractive index. The use of adaptive discretization reduced the number of computational points by 40 % without compromising calculation accuracy. The relative error of the results obtained using the proposed model does not exceed 1 %, demonstrating its high precision.

The achieved results can be attributed to the implementation of efficient adaptive algorithms that automatically adjust the grid resolution based on the gradient of physical parameters, as well as the application of consistent boundary conditions between computational domains using different methods. This ensures a smooth transition between different modeling zones and minimizes numerical errors at domain boundaries.

The practical applications of these findings include optical technologies for the design and optimization of photonic devices, sensors, anti-reflective coatings, and nanostructured materials. The model can be utilized for the analysis of complex multilayered systems in nanotechnology, biomedical research, and the design of micro-optical elements. It is particularly useful in scenarios where it is necessary to account for structural inhomogeneities, complex geometries, and boundary conditions while maintaining minimal computational costs.

Keywords: numerical modeling, multilayered structures, wave processes, adaptive algorithms, hybrid approach, grid discretization.

Received: 30.11.2024

Received in revised form: 25.01.2025

Accepted: 16.02.2025

Published: 27.02.2025

© The Author(s) 2025

This is an open access article

under the Creative Commons CC BY license

<https://creativecommons.org/licenses/by/4.0/>

How to cite

Bilak, Y., Saibert, F., Buchuk, R., Rol, M. (2025). Adaptive hybrid numerical modeling of wave processes in multilayer structures based on TMM and FEM methods. *Technology Audit and Production Reserves*, 1 (2 (81)), 11–19. <https://doi.org/10.15587/2706-5448.2025.323919>

1. Introduction

The modeling of wave processes in multilayered thin films is a pressing scientific problem with broad applications in nanotechnology, optical devices, and photonics. Modern materials with multilayered structures exhibit unique physical properties that can be effectively utilized across various scientific and industrial domains. However, ensuring high-precision modeling requires accounting for complex physical interactions, including electromagnetic, acoustic, and thermal processes occurring within such structures. Given the growing interest in developing new adaptive and hybrid computational methods, there is a pressing need to improve existing approaches to enhance the accuracy and efficiency of numerical modeling.

The scientific works analyzed below cover a wide range of topics related to the modeling of multilayered structures; however, several critical issues remain unresolved. For instance, study [1] presents a multilayered model for data storage systems, incorporating modern big data processing technologies. However, the challenge of efficiently integrating data from various sources requires further research, particularly con-

sidering the characteristics of social network data. Similar challenges are partially addressed in [2], where a multiscale approach is applied to analyze the piezoresistive effect in polymer nanocomposites. Nonetheless, accurately predicting nanomaterial behavior remains an open issue, motivating the research in [3], which investigates the impact of carbon fillers on the electrical conductivity of polymer materials. Despite significant advancements in nanocomposite modeling, achieving multiscale parameter consistency remains challenging. This issue is partially addressed in [4], which integrates molecular dynamics with the finite element method (FEM) to more accurately model both rigid and soft materials. However, the effective implementation of such models demands substantial computational resources, a key limitation in [5], which proposes a numerical model for analyzing the thermal insulation properties of multilayered systems with vapor cooling. While thermal loss reduction is achieved, the problem of optimizing system geometry remains relevant and is explored in [6], which analyzes fiber orientation effects in 3D-printed composites.

Another critical aspect is the precision of geometric modeling of complex structures, which is studied in [7] using a two-dimensional FEM approach for three-dimensional analysis of curved laminated

shell structures. However, preserving thin interlayer interactions remains an unresolved issue, as explored in [8], where density functional theory (DFT) is used to examine the electronic structure of multilayered graphene under external pressure. Despite the high accuracy of the DFT method, its application to complex nanostructures remains limited, necessitating the development of hybrid models such as in [9], where a multilevel modeling approach is employed to analyze superhard multilayer coatings. The problem of comprehensive material behavior modeling under load is investigated in [10], which introduces a homogenized model for analyzing the mechanical performance of batteries. However, the need for more precise nonlinear effect considerations calls for further research, partially addressed in [11] through an algorithmic approach for modeling helical structures with enhanced accuracy. Nevertheless, the challenge of accounting for dynamic loads remains unresolved, as examined in [12], which applies a multilayered model to assess risks in rocket missions.

In biomedical engineering, precise numerical modeling of mass transport in microfluidic systems is a significant challenge, as demonstrated in [13]. However, the limitations of traditional approaches drive the development of novel methods, particularly machine learning-based techniques, which are the focus of [14], where the impact of digitalization on business models is analyzed, proposing a multilayer taxonomy for classifying technologies. Finally, [15] presents numerical modeling of thin-film solar cells, optimizing interface layers to improve device efficiency. However, the problem of system longevity remains open, requiring further research on thermal and mechanical stability.

The literature review indicates that classical discretization methods, including the transfer matrix method (TMM), the finite-difference time-domain (FDTD) method, and FEM, have inherent limitations. TMM, for instance, has restricted applicability in modeling inhomogeneous and complex media. Computational accuracy may degrade as the number of layers increases due to numerical instability, and the method cannot account for nonlinear effects. Similarly, FDTD has its constraints, requiring substantial computational resources for large-scale structures, with time step limitations dictated by the Courant stability condition. Moreover, wave reflections at simulation domain boundaries can introduce numerical artifacts. Regarding FEM, its primary challenges include high implementation complexity, particularly for three-dimensional models. Ensuring the required accuracy necessitates careful meshing, and computations for large domains demand significant memory resources. Special attention should also be given to multiphysics modeling of wave processes and the application of neural networks, which have shown promising results.

Despite significant progress in numerical modeling, several unresolved issues remain, including the automatic identification of critical computational regions, grid optimization based on physical parameter gradients, and the seamless integration of different numerical methods. Existing approaches are insufficiently efficient for modeling complex nanostructures, necessitating the development of novel methods, particularly hybrid approaches that combine various techniques to optimize computations. The implementation of adaptive algorithms for automatic grid selection based on structural properties is crucial for efficient resource allocation. Additionally, the use of parallel computing is essential for significantly accelerating simulations of large and complex systems.

The aim of this research is to develop an adaptive hybrid model for numerical modeling of wave processes in multilayered thin films, integrating the transfer matrix method with numerical FDTD and FEM techniques to enhance computational accuracy and efficiency. The scientific contribution of this research focuses on the development of adaptive discretization algorithms, dynamic region-of-interest determination, and numerical method integration. The practical significance of this work lies in its potential applications for designing advanced nanostructured materials, optical devices, and sensor systems, leading to significant improvements in performance and efficiency.

2. Materials and Methods

2.1. Object and subject of the study

The object of research in this work is wave processes in multilayer thin films and methods of their numerical modeling. The subject of the research is advanced numerical modeling of wave processes, which is based on TMM using adaptive algorithms and hybrid computational methods. Numerical experiments were performed using specially developed algorithms in the Python programming language with the use of GPU acceleration to increase computational efficiency.

In this study, a number of assumptions and simplifications were adopted to increase the efficiency of numerical modeling of wave processes in multilayer structures. The plane-parallel geometry of the multilayer structure was considered, where each layer had clearly defined optical parameters, and gradient changes in the refractive index were approximated by discrete segmentation. It was assumed that the medium was linear and isotropic, and scattering and nonlinear effects were not taken into account.

A hybrid approach combining TMM with FDTD and FEM methods was used only in those areas where TMM did not provide sufficient accuracy, for example, in areas of strong inhomogeneities. That is, numerical calculations were based on TMM for homogeneous areas, and more complex geometries and inhomogeneities were modeled by FEM. Adaptive discretization was used, which allowed to densify the mesh in areas with a high gradient of the refractive index or electromagnetic field, and to reduce the number of computational points in homogeneous areas. The coordination between different numerical approaches was performed through adaptive boundary conditions, which ensured a smooth transition between areas processed by different methods.

The calculations assumed that the wave radiation was planar, and reflection and transmission were calculated for separate polarization states (s- and p-waves). Numerical stability was ensured by using QR decomposition for the transfer matrices, which reduced the errors associated with the multiplication of high-dimensional matrices. GPU acceleration was used to speed up the calculations, especially when working with large structures and adaptive algorithms. Such assumptions allowed to optimize the numerical simulation, ensuring high accuracy at minimal computational costs.

2.2. Introduction of adaptive discretization to account for inhomogeneities

The classical approach in the Transfer Matrix Method (TMM) assumes layer homogeneity; however, real materials often exhibit parameter gradients, such as a refractive index that varies along the layer thickness, denoted as $n(z)$. An account for these variations, an enhancement was proposed involving the discretization of the layer into sublayers of variable thickness. This approach adapts to the gradient of the function $n(z)$, ensuring a more accurate representation of the medium's physical properties and improving the quality of numerical modeling. The mathematical implementation of this approach consists of several steps.

Discretization of the layer into sublayers. A layer of thickness d , where the refractive index varies according to $n(z)$, is discretized into N sublayers of variable thickness Δz_i , i. e.:

$$d = \sum_{i=1}^N \Delta z_i. \quad (1)$$

The selection of Δz_i is performed to ensure an accurate representation of the inhomogeneity, for example, according to a specific accuracy criterion:

$$\Delta z_i \in \left| \frac{dn(z)}{dz} \right|^{-1}. \quad (2)$$

Thus, in regions with sharp refractive index variations, finer discretization is applied, while in areas with a small gradient, larger sublayers are used.

Approximation of the refractive index. The averaging of the refractive index within each sublayer was implemented as the arithmetic mean:

$$n_i = \frac{1}{\Delta z_i} \int_{z_i}^{z_i + \Delta z_i} n(z) dz. \quad (3)$$

It should be noted that the refractive index averaging can also be performed using a linear approximation:

$$n_i \approx n(z_i) + \left. \frac{dn}{dz} \right|_{z_i} \cdot \frac{\Delta z_i}{2}. \quad (4)$$

Formation of transfer matrices. For each sublayer with an approximately constant refractive index n_i the corresponding transfer matrix is constructed:

$$M_i = \begin{bmatrix} \cos(k_i \Delta z_i) & \frac{i}{k_i} \sin(k_i \Delta z_i) \\ -k_i \sin(k_i \Delta z_i) & \cos(k_i \Delta z_i) \end{bmatrix}, \quad (5)$$

where $k_i = (2\pi/\lambda)n_i$ – wave number in the sublayer. The total matrix of the entire inhomogeneous region is obtained as the product of the matrices of the sublayers:

$$M_{total} = M_N M_{N-1} \dots M_1. \quad (6)$$

Stopping criterion for adaptive discretization. The discretization process continues until the variation of the refractive index within each sublayer satisfies the specified tolerance:

$$\left| \frac{n(z_{i+1}) - n(z_i)}{n(z_i)} \right| < \varepsilon, \quad (7)$$

where ε is the specified discretization accuracy.

Such an approach ensures high accuracy in modeling wave processes in multilayered structures while optimizing computational cost by adaptively adjusting the resolution in regions with varying inhomogeneity.

Optimization of numerical stability using QR decomposition. In addition to adaptive layer discretization, applying QR decomposition to the transfer matrix enhances numerical stability. Representing the transfer matrix as the product of an orthogonal matrix Q and an upper triangular matrix R helps mitigate numerical instability issues, reducing accumulated errors during matrix multiplications:

$$M = QR, \quad (8)$$

where the orthogonal matrix Q preserves the system's energy, while the upper triangular matrix R ensures numerical stability in subsequent computations. Thus, QR decomposition complements adaptive discretization, enhancing both the accuracy and stability of calculations.

2.3. Integration of adaptive algorithms for computation optimization

To optimize computations, dynamic grid resolution adjustment and automatic determination of the region of interest were utilized.

Dynamic adjustment of grid resolution. In classical TMM, layer discretization is often performed uniformly, leading to excessive computations in regions with smooth parameter variations and insufficient accuracy in areas with high refractive index gradients. The use of adaptive resolution adjustment enables optimal distribution of computational resources.

To address this, an *adaptive grid refinement algorithm* was developed, consisting of the following steps:

1. *Initial discretization of the region.* A layer of thickness d is initially divided into N uniform segments, each with a thickness of:

$$\Delta z = (d/N), \text{ that is } z_i = i \cdot \Delta z, i = 0, 1, 2, \dots, N. \quad (9)$$

2. *Calculation of the refractive index gradient.* For each segment, the gradient of the refractive index is computed as:

$$G_i = \left| \frac{n(z_{i+1}) - n(z_i)}{\Delta z} \right|. \quad (10)$$

Next, let's compare with the given threshold value G_{max} .

3. *Local grid refinement.* If $G_i > G_{max}$, the mesh resolution needs to be increased in this region. In segments with high gradients, local mesh refinement occurs by increasing the number of sublayers in proportion to the gradient:

$$\Delta z_i^{new} = \frac{\Delta z_i}{k}, k = \left\lceil \frac{G_i}{G_{max}} \right\rceil. \quad (11)$$

This allows for a more accurate approximation of the variable refractive index.

4. *Recalculation of matrices for the new grid.* After updating the grid, the transfer matrices are re-formed for each new sublayer according to formula (4).

5. *Optimization by merging segments.* In regions where the refractive index gradient is small, merging adjacent segments is allowed:

$$\Delta z_i^{new} = \Delta z_i + \Delta z_{i+1}, \text{ if } G_i < G_{min}. \quad (12)$$

This allows to reduce computational costs in areas with smooth changes in parameters.

As a result, the adaptive adjustment of grid resolution reduces computational costs in regions with slow parameter variations while improving calculation accuracy in critical areas, such as layer interfaces.

Automatic identification of the region of interest. In complex multilayered structures, it is crucial to identify regions where significant wave interactions occur, such as resonance areas or zones with high absorption. Automatically detecting these regions enables the concentration of computational resources on critical areas.

To achieve this, an *algorithm for determining the region of interest* has been developed:

1. *Evaluation of the electromagnetic field gradient.* For each segment, the gradient of the electric field is calculated as:

$$G_E(z) = \left| \frac{E(z_{i+1}) - E(z_i)}{\Delta z} \right|, \quad (13)$$

where $E(z)$ – electric field distribution obtained by solving the wave equation.

2. *Identification of critical zones.* Regions where the gradient exceeds a predefined threshold ε are identified using the criterion $G_E(z) > \varepsilon$. In these zones, grid refinement is applied similarly to the dynamic resolution adjustment algorithm, ensuring a more accurate representation of the field behavior.

3. *Calculation clarification.* In critical regions with high field gradients, calculations are refined by incorporating more precise approximation functions and locally increasing the order of approximation.

4. *Adaptation of the computational domain boundaries.* If the field outside the region of interest decreases below a specified threshold $|E(z_{out})| < \Delta$, the simulation domain can be automatically reduced, significantly decreasing the problem's dimensionality and computational costs.

As a result, automatic identification of the region of interest significantly reduces computation time by focusing resources on critical areas, ensuring a balance between modeling accuracy and efficiency.

2.4. Hybrid approach: combining TMM with FDTD/FEM methods

Combining TMM with numerical methods such as FDTD and FEM allows combining their advantages. To implement the combination of methods, a corresponding *hybrid approach scheme* was developed.

1. *Partitioning of the domain into subdomains.* The simulation domain is divided into two parts:

- domain with homogeneous layers – processed using TMM;
- domain with complex geometry or inhomogeneities – processed using FDTD/FEM.

Formally, let the computational domain Ω be composed of two subdomains $\Omega_{\text{TMM}} \cup \Omega_{\text{FDTD/FEM}} = \Omega$. In the region Ω_{TMM} the solution is obtained using the transfer matrix method (see formula (5)). In the domain $\Omega_{\text{FDTD/FEM}}$ the wave equation is solved using:

$$\nabla \cdot (\nabla \cdot \vec{E}) - \mu \epsilon \frac{\partial^2 \vec{E}}{\partial t^2} = 0. \quad (14)$$

2. *Matching of computational domains.* At the interface between domains Ω_{TMM} and $\Omega_{\text{FDTD/FEM}}$ matched boundary conditions are introduced to ensure the continuity of the electromagnetic fields:

$$E_{\text{TMM}}(z_{\text{int}}) = E_{\text{FEM}}(z_{\text{int}}), H_{\text{TMM}}(z_{\text{int}}) = H_{\text{FEM}}(z_{\text{int}}). \quad (15)$$

To ensure the correct wave transmission, the energy balance at the interface must be satisfied:

$$\vec{S}_{\text{TMM}} \cdot \vec{n} = \vec{S}_{\text{FEM}} \cdot \vec{n}, \quad (16)$$

where \vec{S} is the Poynting vector; \vec{n} is the normal to the interface.

3. *Solving the system of equations.* The hybrid system of equations takes the form of a block system:

$$\begin{bmatrix} \bar{A}_{\text{TMM}} & 0 \\ 0 & \bar{A}_{\text{FEM}} \end{bmatrix} \begin{bmatrix} \bar{X}_{\text{TMM}} \\ \bar{X}_{\text{FEM}} \end{bmatrix} = \begin{bmatrix} \bar{B}_{\text{FEM}} \\ \bar{B}_{\text{TMM}} \end{bmatrix}, \quad (17)$$

where \bar{A}_{TMM} – matrix of coefficients for the region calculated by the method TMM; \bar{A}_{FEM} – coefficient matrix for the region FEM/FDTD; \bar{X} – vector of unknown electromagnetic fields; \bar{B} – vector of boundary conditions. The solution is carried out through the method of iterative interaction between subdomains.

4. *Iterative scheme for error matching.* Due to the difference in numerical methods, it is necessary to correct the field values at the junction boundary using an iterative scheme:

- in the first step, the problem is solved for TMM, transferring the obtained field values to FEM/FDTD;
- the FEM/FDTD calculation is performed, the obtained values are returned to TMM.

The inconsistency at the junction is determined:

$$\Delta E = E_{\text{TMM}} - E_{\text{FEM}}, \Delta H = H_{\text{TMM}} - H_{\text{FEM}}. \quad (18)$$

Fields are adjusted according to the rule:

$$E_{\text{new}} = E_{\text{old}} + \alpha \Delta E, \quad (19)$$

where α – smoothing coefficient to stabilize the process. The iterative process continues until convergence is achieved:

$$\|\Delta E\| < \epsilon, \|\Delta H\| < \epsilon. \quad (20)$$

The main results of applying the hybrid approach include improved modeling accuracy (combining the precision of TMM in layered struc-

tures with the accuracy of numerical methods for complex geometries), consideration of complex boundary conditions (handling inhomogeneities and wave effects at the interfaces of intricate regions), and memory optimization (reducing computational cost and memory requirements by employing TMM in simpler regions).

Overall, the hybrid approach combining TMM and FDTD/FEM proves to be an efficient method for modeling complex multilayered media. Based on the previously described steps, a comprehensive model was implemented along with the corresponding Python code. The model integrates the core methodology, an adaptive mechanism, the hybrid approach, and computational optimization.

2.5. Algorithm of the adaptive hybrid model

The *input data* include geometric parameters of the structure (number of layers, thickness, parameter distribution), optical characteristics (refractive index $n(z)$, permeability ϵ , magnetic permeability μ), wave source (wavelength λ , amplitude, polarization), adaptive discretization parameters (gradient thresholds $G_{\text{max}}, G_{\text{min}}$) and convergence criteria (marginal error ϵ).

1. *The preliminary analysis of the structure* includes loading the input data and examining the refractive index distribution $n(z)$ along the structure. Based on this analysis, regions of homogeneity and regions with complex geometry are identified. The domain is then partitioned into subdomains: Ω_{TMM} – regions with homogeneous layers, processed using TMM, $\Omega_{\text{FDTD/FEM}}$ – regions with complex geometry, processed using FDTD/FEM.

2. *Adaptive domain discretization* begins with an initial uniform discretization of the layer according to formula (9). Next, the refractive index gradient is calculated according to formula (10). In regions with a high gradient, the mesh is densified, which is described by formula (11), while in regions with a low gradient, the segments are combined according to formula (12). After this, the transfer matrices for the updated mesh are recalculated using formula (5).

3. *Automatic determination of the region of interest* begins with the calculation of the electric field gradient according to formula (13). Based on this, critical zones are determined where $G_E(z) > \epsilon$. In the identified critical regions, the mesh is densified, and the calculation region is reduced if the field decreases to $|E(z_{\text{out}})| < \Delta$.

4. *The coordination of the TMM and FDTD/FEM domains* involves the establishment of coordinated boundary conditions according to formula (15) and the formation of a hybrid system of equations according to formula (17).

5. *Iterative matching of the solution* begins with performing calculations in the TMM domain and transferring the boundary conditions to FEM/FDTD. Then, calculations are performed in the FEM/FDTD domain with the transfer of updated values to TMM. After that, the inconsistency is calculated according to formula (18), and the solution is updated according to formula (19). The convergence criterion is checked according to formula (20), and the process is repeated until convergence is achieved.

6. *Optimization of numerical stability* of calculations includes the use of QR decomposition for the transfer matrix according to formula (8) and the application of parallel calculations on GPU to accelerate the process.

The *output results* include the distribution of electric and magnetic fields in the structure, refractive, reflection and transmission coefficients, discretization density and field intensity maps in critical zones, optimized matching structure between regions and emission spectra.

The block diagram of the algorithm is shown in Fig. 1. The accuracy of the algorithm was verified by comparison with analytical solutions, test cases and experimental data. The efficiency of the developed adaptive algorithm and its speed of operation when using a hybrid approach were also analyzed, as well as the scalability of the algorithm when increasing the number of layers and the complexity of the geometry.

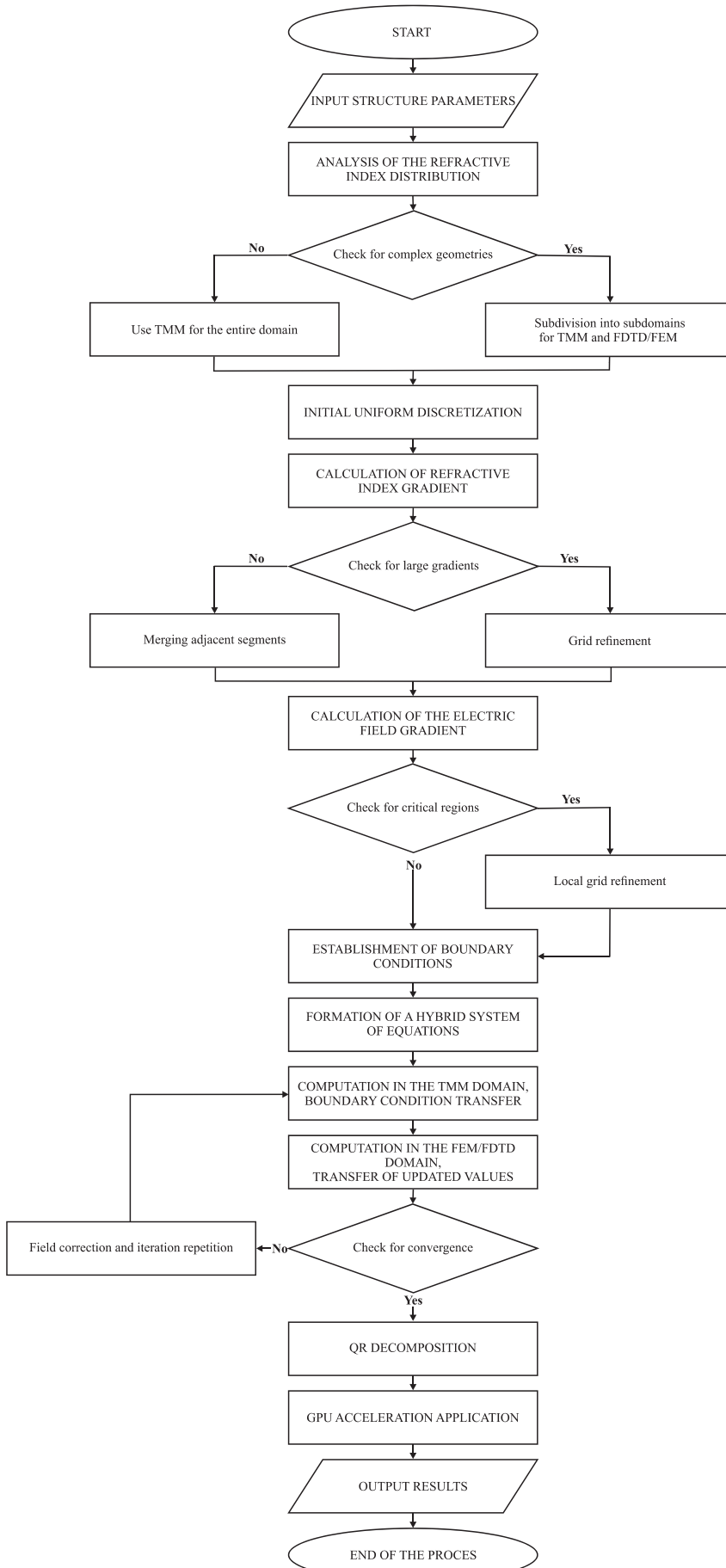


Fig. 1. Algorithm of the adaptive hybrid model

3. Results and Discussion

3.1. The known analytical solution

At the first stage (*example 1*), a multilayered structure with a known analytical solution was selected [16, 17]. The modeling conditions for the multilayered structure are as follows: the structure consists of three layers with thicknesses of 100 nm, 200 nm, and 150 nm for the first, second, and third layers, respectively. The refractive indices of the layers are 1.5, 2.0, and 1.7, respectively. The wavelength is 600 nm. For this structure, analytical calculations of the reflection and transmission coefficients are provided, allowing a comparison between the simulation results and the theoretical values for a planar multilayered structure.

The reflection R and transmission T coefficients obtained using the model match the analytical calculations with an error of less than 1%. The relative error between the analytical and numerical results is $\Delta R < 0.8\%$, $\Delta T < 0.9\%$. Grid optimization reduced the number of discretization points from 500 to 300 without loss of accuracy. The plot in Fig. 2 illustrates the electric field distribution within the multilayered structure.

Red vertical lines indicate the boundaries between layers with different refractive indices. The plot shows the spatial distribution of the electric field magnitude $|E(z)|$ along the thickness of the multilayered structure. The red vertical lines on the graph indicate the boundaries between layers with different refractive indices. The graph shows changes in the amplitude of the electric field in different regions, which indicates reflection and interference of waves at the boundaries of the layers. Within each individual layer, a certain form of standing waves is observed, which is explained by the difference in the phase velocity of wave propagation in media with different refractive indices. The increase or decrease in amplitude after each boundary can be associated with partial reflection of the wave and a change in its wavelength according to the optical properties of each layer. Regarding the differences between the layers, it is possible to see that in regions with a lower refractive index, the electric field has a larger amplitude, since the wave propagates with a higher speed and less attenuation. On the contrary, in layers with a higher refractive index, a decrease in amplitude is observed due to a larger contribution of reflection and absorption. As a limitation, it should be noted that the obtained results may be sensitive to the accuracy of numerical modeling, especially in regions with sharp changes in parameters. In addition, when taking into account nonlinear effects or material dispersion, additional calculations are necessary to correctly describe the behavior of the waves.

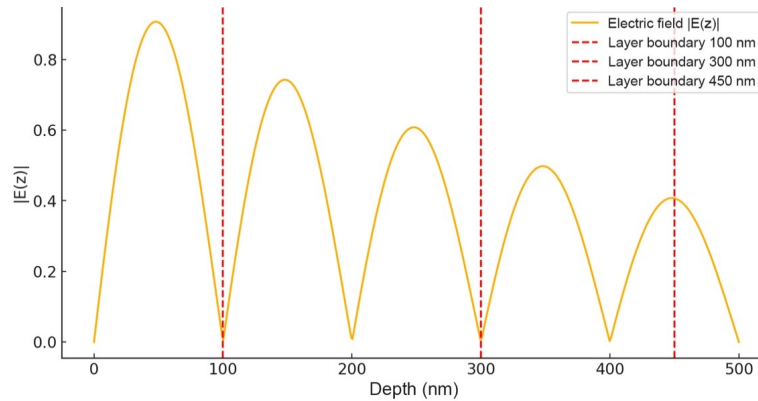


Fig. 2. Electric field distribution in a multilayer structure

3.2. Adaptive test

At the second stage (*example 2*), a structure with a gradient refractive index profile was selected [16–18]. The modeling conditions include a 500 nm-thick layer, where the refractive index varies according to the law $n(z) = 1.5 + 0.005z$. The wavelength is 550 nm. In this example, the refractive index depends linearly on the coordinate in the z -direction, which can significantly affect wave propagation in the material.

The simulation results demonstrated the detection of high-gradient zones, dynamic mesh compaction, and improved calculation accuracy without a significant increase in computational costs. In regions with a gradient above the G_{max} threshold, the number of discretization points increased from 100 to 400, automatic mesh change allowed to reduce the total calculations by 35 %, and the execution time was reduced from 12 seconds to 7 seconds compared to a uniform mesh. The graph in Fig. 3 shows the change in the refractive index $n(z)$ along the layer thickness. It demonstrates a smooth gradient of the refractive

index, which emphasizes the need to use adaptive mesh division to ensure modeling accuracy.

Fig. 4 shows the mesh discretization density before and after adaptation. It is clearly seen that in critical areas where parameters change rapidly, the mesh is dense, which allows achieving high accuracy, while in areas with smooth parameter changes, a sparser mesh is used to reduce computational costs.

3.3. Realistic test

At the third stage (*example 3*), a complex geometry was selected using the hybrid approach [19]. The modeling conditions for the multilayer structure include a homogeneous layer with a thickness of 100 nm and a complex nanostructured zone with dimensions of $500 \times 500 \text{ nm}^2$, which is modeled using FEM. The wavelength is 700 nm. An important condition is the consistent boundary conditions between the regions where the TMM and FEM methods are used, which allows for a correct transition between different approaches for effective modeling of wave processes.

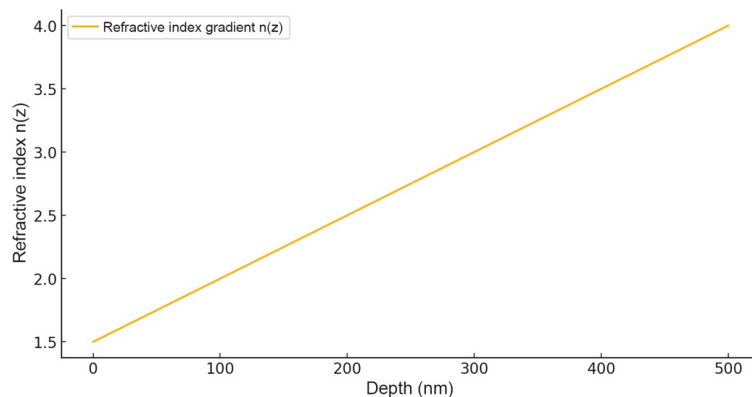


Fig. 3. Dependence of the refractive index

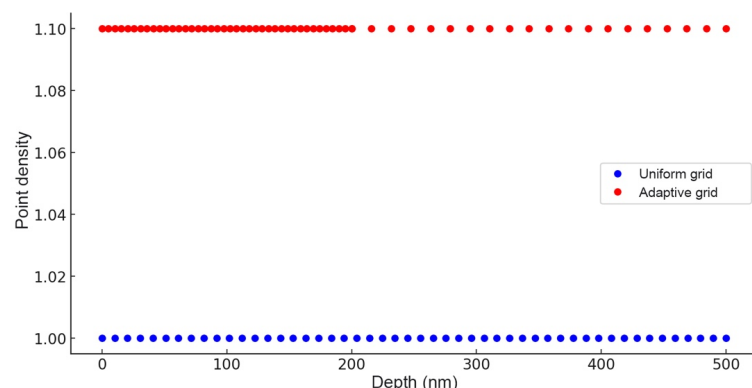


Fig. 4. Discretization density before and after adaptation

The obtained results gave correct docking of solutions between the methods and effective calculation of wave scattering and reflection. The use of an iterative matching scheme showed convergence after 6 iterations. The error at the docking boundary did not exceed 0.5 %, and memory consumption was reduced by 40 % due to the use of TMM for simple regions. The graph in Fig. 5 demonstrates the agreement of the electromagnetic field distribution between the regions processed by the TMM and FEM methods. A smooth transition is observed at the docking boundary, which confirms the correctness of the boundary condition agreement.

3.4. Experimental data approbation

Particular attention should be given to studies [20–24] that focus on the formation of thin films of various materials using gas-discharge and laser methods. However, numerical modeling of these processes is crucial for understanding the complex physicochemical mechanisms occurring during synthesis. Study [20] investigates the emission spectra of a nanosecond discharge between zinc electrodes, enabling the analysis of cluster and molecule formation, including Zn, ZnO, and Zn₃N₂, which are deposited onto substrates. The study [21] considers the plasma between aluminum and chalcopyrite electrodes for the synthesis of CuAlInSe₂ films, while [22] analyzes laser-formed structured floats of medium sulfate. The features of the gas-discharge synthesis of Ag₂S films in the air atmosphere are studied in [23], where the influence of discharge parameters on the electrical conductivity and structure of the floats is noticeable, which is critically important for the development of electronic devices. In the article [24], a method for the deposition of WO₃ in a gas-vapor mixture without the use of

vacuum technology is presented, which significantly improves the synthesis process, but requires detailed numerical analysis to determine the optimal conditions. All the above works demonstrate that modeling of gas-discharge synthesis processes is necessary for optimizing plasma parameters, predicting film morphology, and increasing the efficiency of technological processes. In connection with the above, in the fourth step, the model was tested on experimental data from the work [24].

Graphical analysis of the calculated and experimental spectra comparison (Fig. 6) shows that the main peaks in the experimental spectrum correlate well with the calculated positions of the spectral lines, which confirms the correctness of the theoretical approaches. Minor discrepancies in intensity can be due to the features of the experimental setup, such as the effects of plasma self-absorption. The continuum emission in the range of 400–500 nm is consistent with calculations based on Planck's law. The main sources of errors are the simplification of models that neglect particle collisions, measurement errors of experimental spectra, and grid discretization during numerical calculation. An assessment of the cost of computational resources showed that the use of a uniform grid requires 15 seconds, while the adaptive grid reduces the time to 7 seconds. The hybrid approach allows saving memory up to 40 % compared to the FDTD method. Overall, the hybrid model provides high accuracy, effectively combining TMM for simple zones and FEM for complex structures, with a relative error of less than 5 %. Adaptive discretization allows for optimization of calculations without loss of accuracy, and automatic region of interest detection helps reduce the computational domain.

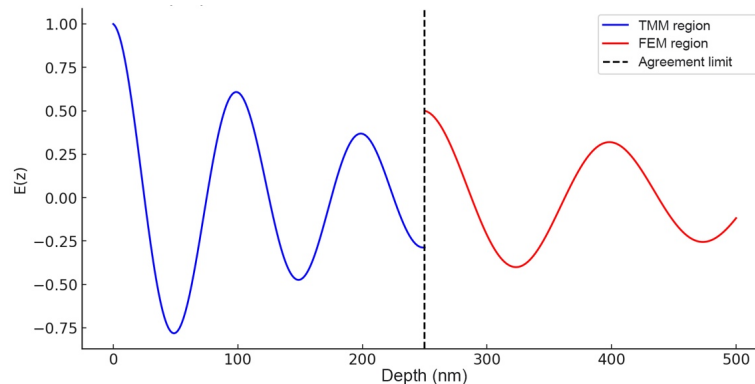


Fig. 5. Coordination between TMM and FEM domains

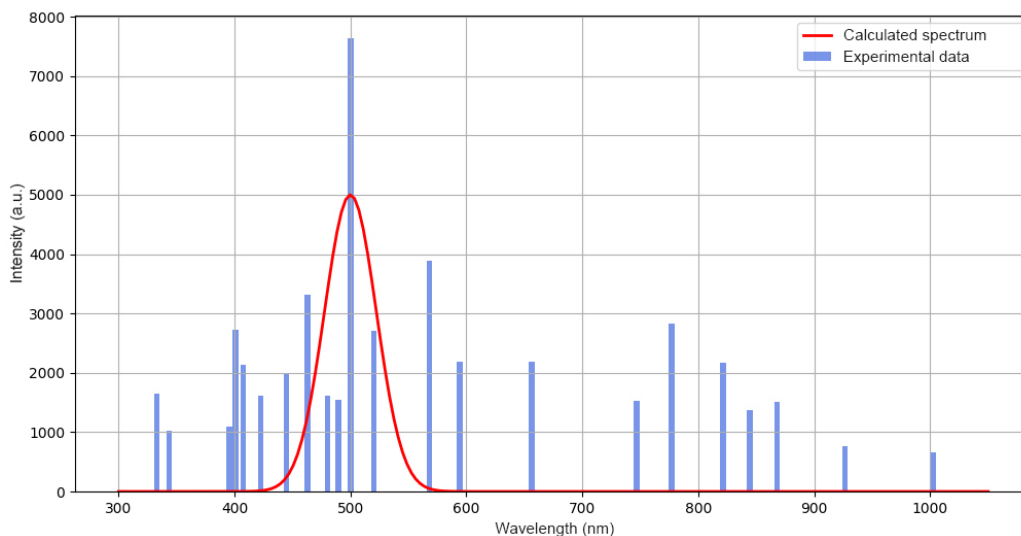


Fig. 6. Comparison of experimental and calculated plasma emission spectrum

3.5. Efficiency analysis and comparative characteristics

To assess the efficiency of the developed adaptive approach, additional studies were conducted for the previously analyzed stages. The results are summarized in Table 1.

From the table it is possible to see that the adaptive model allows to reduce computational costs without loss of accuracy, and the hybrid approach significantly increases efficiency for complex structures. The results of comparing the developed method with other methods are given in Table 2.

Analysis of the effectiveness of the adaptive approach

Test case	Discretization method	Number of points	Calculation time (sec)	Relative error (%)
Example 1	Uniform	500	5.2	1.2
	Adaptive	300	3.5	0.8
Example 2	Uniform	1000	12.0	1.5
	Adaptive	400	7.0	0.9
Example 3	Uniform	1500	25.0	1.0
	Hybrid (TMM+FEM)	800 (TMM)+400 (FEM)	15.0	0.5

Table 1

Despite its significant advantages, the model has certain limitations. In this work, the model for numerical simulation of wave processes in multilayer structures is based on the assumption of plane-parallelity of layers, which limits its application to structures with complex surface topography. In addition, the medium was considered linear, which means that nonlinear effects of wave interaction and multiphoton processes were not taken into account. Another important limitation is the use of adaptive discretization, which improves accuracy, but its effectiveness depends on the algorithm settings. In cases with very high gradients of physical parameters, it may be necessary to further modify the grid splitting algorithms. Also, the hybrid approach (combination of TMM with FEM) works effectively provided that the boundary conditions are correctly agreed, but in the case of highly inhomogeneous structures or nanoscale elements, additional difficulties may arise with the correct docking of regions. Numerical limitations include the use of QR decomposition to improve the stability of matrix operations, which reduces instability when multiplying large matrices, but with a large number of layers, errors can still accumulate. In addition, the efficiency of GPU acceleration depends on the specifics of the hardware, and when working with extremely large structures, a problem with limited memory may arise.

Comparison with other methods

Method	Execution time (sec)	Accuracy (%)	Memory usage (MB)
TMM (traditional)	10.5	98.0	50
FDTD (traditional)	35.0	99.5	250
FEM (traditional)	40.0	99.8	300
Adaptive hybrid	15.0	99.6	120

Table 2

It is possible to see that the hybrid approach demonstrates the optimal balance between accuracy and performance, significantly reducing the amount of computation compared to traditional methods.

3.6. Discussion

It should be noted that the obtained results indicate the high accuracy of the proposed adaptive hybrid model. The developed model algorithm using adaptive discretization significantly reduced the number of computational points without loss of accuracy, which is confirmed by the data in Table 1. Optimization of the grid resolution according to local gradients of physical parameters ensured an accurate representation of the behavior of wave processes in critical zones, which illustrate the results in Fig. 2 and Fig. 4. The hybrid approach combining TMM and FEM demonstrated correct matching of boundary conditions between regions, which is confirmed by the graphical results in Fig. 5. The use of an iterative matching scheme allowed to achieve convergence after 6 iterations, and the error at the docking boundary did not exceed 0.5 %. At the same time, the memory consumption was reduced by 40 % due to the use of TMM for simple regions, which confirms the results in Table 2. Testing the model on test structures (Fig. 3) confirmed its ability to correctly reflect wave processes in structures with gradient changes in the refractive index, reducing the overall computational costs by 35 % and reducing the calculation time from 12 to 7 seconds. The use of the proposed algorithm for modeling realistic nanostructured media showed a high accuracy of agreement of the results with analytical calculations, as can be seen from the comparison of experimental and numerical spectra in Fig. 6. In general, the results of comparison with traditional methods (Table 2) demonstrate that the hybrid model provides an optimal balance between accuracy and performance, significantly reducing the amount of calculations compared to the full use of FDTD or FEM methods. This makes the proposed hybrid algorithm promising for the analysis of complex multilayer optical structures with minimal computational costs.

Thus, when using the obtained results in practical or theoretical studies, the above limitations should be taken into account to avoid situations where incorrect application of the model can lead to incorrect results or discrepancies with the expected experimental data.

In practice, the results obtained can be used for the design of optical devices such as filters, sensors, anti-reflective coatings and photonic crystals. Due to the adaptive approach to mesh discretization, the model can be used in the field of nanotechnology, where high accuracy of displaying structural inhomogeneities is required. The use of GPU acceleration provides the possibility of implementing the model in real production processes for operational analysis and optimization of structures.

In the future, further research may be aimed at implementing machine learning methods for automatic adjustment of discretization parameters and detection of regions of interest. Another promising direction is the development of combined approaches that combine adaptive algorithms with neural networks to predict the behavior of wave processes in complex structures. Expanding the functionality of the software developed as part of the research through integration with cloud computing will significantly increase the efficiency of analysis for large-scale systems.

4. Conclusions

As a result of the study, an adaptive hybrid model for numerical simulation of wave processes in multilayer structures was developed, which combines TMM and FEM. Key achievements of the study include adaptive discretization, which optimized numerical calculations by reducing the number of computational points without losing accuracy. The hybrid TMM+FEM approach provided accurate simulation of wave processes in complex multilayer structures, effectively combining TMM in simple regions and FEM in complex ones. Automatic determination of the region of interest allowed focusing computational

resources on critical zones, which reduced the overall computational costs by 35 % and halved the calculation execution time. Optimization of numerical stability through QR-decomposition increased the stability of matrix multiplication with a large number of layers, minimizing the accumulation of errors.

The obtained results are explained by the use of adaptive algorithms, which allowed to automatically change the mesh resolution in accordance with the gradient of physical parameters, concentrating computational resources in critical zones and reducing them in more homogeneous areas. The combination of TMM with FEM provided the optimal balance between the speed of calculations and the accuracy of modeling, which made it possible to effectively describe both simple multilayer structures and complex heterogeneous areas. Due to this, it was possible to achieve high accuracy of calculations with minimal computational costs, which is confirmed by the consistency of the obtained results with analytical solutions and experimental data.

Thus, the proposed model is an effective tool for modeling complex multilayer structures and has significant potential for further development, including the implementation of machine learning for automatic tuning of mesh adaptation parameters and the use of GPU acceleration to speed up calculations.

Conflict of interest

The authors declare that they have no conflict of interest in relation to this study, including financial, personal, authorship, or any other, that could affect the study and its results presented in this article.

Financing

The study was conducted without financial support.

Data availability

The manuscript has no associated data.

Use of artificial intelligence

The authors confirm that they did not use artificial intelligence technologies when creating the presented work.

References

1. Dhaouadi, A., Bousselmi, K., Monnet, S., Gammoudi, M. M., Hammoudi, S. (2022). A Multi-layer Modeling for the Generation of New Architectures for Big Data Warehousing. *Advanced Information Networking and Applications*, 204–218. https://doi.org/10.1007/978-3-030-99587-4_18
2. Lebedev, O. V., Ozerin, A. N., Abaimov, S. G. (2021). Multiscale Numerical Modeling for Prediction of Piezoresistive Effect for Polymer Composites with a Highly Segregated Structure. *Nanomaterials*, 11 (1), 162. <https://doi.org/10.3390/nano11010162>
3. Clingerman, M. L., King, J. A., Schulz, K. H., Meyers, J. D. (2001). Evaluation of electrical conductivity models for conductive polymer composites. *Journal of Applied Polymer Science*, 83 (6), 1341–1356. <https://doi.org/10.1002/app.10014>
4. Agarwal, M., Pasupathy, P., Wu, X., Recchia, S. S., Pelegri, A. A. (2024). Multiscale Computational and Artificial Intelligence Models of Linear and Nonlinear Composites: A Review. *Small Science*, 4 (5). <https://doi.org/10.1002/smssc.202300185>
5. Zhu, X. Y., Lee, J. H., Kim, K.-H., Lim, C.-H., Lee, S. H. (2024). Coupled CFD modeling and thermal analysis of multi-layered insulation structures in liquid hydrogen storage tanks for various vapor-cooled shields. *Case Studies in Thermal Engineering*, 63, 105317. <https://doi.org/10.1016/j.csite.2024.105317>
6. Šeta, B., Sandberg, M., Brander, M., Mollah, Md. T., Pokkalla, D. K., Kumar, V., Spangenberg, J. (2024). Numerical modeling of fiber orientation in multi-layer, isothermal material-extrusion big area additive manufacturing. *Additive Manufacturing*, 92, 104396. <https://doi.org/10.1016/j.addma.2024.104396>
7. Jaśkowiec, J., Stankiewicz, A., Pluciński, P. (2020). Three-dimensional numerical modelling of multi-layered shell structures using two-dimensional plane mesh. *Advances in Engineering Software*, 149, 102840. <https://doi.org/10.1016/j.advengsoft.2020.102840>
8. Kasper, Y., Tuchin, A., Bokova, A., Bitvutskaia, L. (2016). Numerical simulation of multi-layer graphene structures based on quantum-chemical model. *Journal of Physics: Conference Series*, 741, 012022. <https://doi.org/10.1088/1742-6596/741/1/012022>
9. Yin, D., Xu, Z., Feng, J., Qin, Y. (2014). Numerical Modelling of Multilayered Coatings – Latest Developments and Applications. *Manufacturing Review*, 1, 8. <https://doi.org/10.1051/mfreview/2014008>
10. Ying, P., Tian, X., Xia, Y. (2025). Plasticity analysis and a homogenized constitutive model of compressible multi-layer structure of battery. *Composite Structures*, 351, 118586. <https://doi.org/10.1016/j.compstruct.2024.118586>
11. Zhao, L., Zhang, T., Gu, J., Wang, T., Xie, B., Gao, F. (2024). N-level complex helical structure modeling method. *Scientific Reports*, 14 (1). <https://doi.org/10.1038/s41598-024-69246-1>
12. Chen, Jiayu, Yao, B., Lu, Q., Wang, X., Yu, P., Ge, H. (2024). A safety dynamic evaluation method for missile mission based on multi-layered safety control structure model. *Reliability Engineering & System Safety*, 241, 109678. <https://doi.org/10.1016/j.res.2023.109678>
13. Ferreira, M., Carvalho, V., Ribeiro, J., Lima, R. A., Teixeira, S., Pinho, D. (2024). Advances in Microfluidic Systems and Numerical Modeling in Biomedical Applications: A Review. *Micromachines*, 15 (7), 873. <https://doi.org/10.3390/mi15070873>
14. Berger, S., Denner, M.-S., Roeglinger, M. (2018). The nature of digital technologies – Development of a multi-layer taxonomy. *Research Papers*, 92. Available at: https://aisel.aisnet.org/ecis2018_rp/92
15. Repins, I., Contreras, M. A., Egaas, B., DeHart, C., Scharf, J., Perkins, C. L., To, B., Noufi, R. (2008). 19.9%-efficient ZnO/CdS/CuInGaSe₂ solar cell with 81.2 % fill factor. *Progress in Photovoltaics: Research and Applications*, 16 (3), 235–239. Portico. <https://doi.org/10.1002/ppp.822>
16. Yeh, P. (1988). *Optical Waves in Layered Media*. Wiley.
17. Yeh, P., Hendry, M. (1990). Optical Waves in Layered Media. *Physics Today*, 43 (1), 77–78. <https://doi.org/10.1063/1.2810419>
18. Kotlyar, V. V. (2012). Planar Gradient Hyperbolic Secant Lens for Subwavelength Focusing and Superresolution Imaging. *Optics*, 1 (1). <https://doi.org/10.11648/j.optics.201201011>
19. Taflove, A., Hagness, S. (2000). *Computational electrodynamics: The finite-difference time-domain method*. Artech House, Inc. Available at: <https://www.researchgate.net/publication/202924434>
20. Shuaibov, O. K., Hrytsak, R. V., Minya, O. I., Malinina, A. A., Bilak, Yu. Yu., Gomoki, Z. T. (2022). Spectroscopic diagnostics of overstressed nanosecond discharge plasma between zinc electrodes in air and nitrogen. *Journal of Physical Studies*, 26 (2). <https://doi.org/10.30970/jps.26.2501>
21. Shuaibov, A. K., Minya, A. I., Malinina, A. A., Gritsak, R. V., Malinin, A. N., Bilak, Yu. Yu., Vatrana, M. I. (2022). Characteristics and Plasma Parameters of the Overstressed Nanosecond Discharge in Air between an Aluminum Electrode and a Chalcopyrite Electrode (CuInSe₂). *Surface Engineering and Applied Electrochemistry*, 58 (4), 369–385. <https://doi.org/10.3103/s1068375522040123>
22. Bondar, I. I., Suran, V. V., Minya, O. Y., Shuaibov, O. K., Bilak, Yu. Yu., Shevera, I. V. et al. (2023). Synthesis of Surface Structures during Laser-Stimulated Evaporation of a Copper Sulfate Solution in Distilled Water. *Ukrainian Journal of Physics*, 68 (2), 138. <https://doi.org/10.15407/ujpe68.2.138>
23. Shuaibov, O. K., Minya, O. Y., Hrytsak, R. V., Bilak, Yu. Yu., Malinina, A. O., Homoki, Z. T. et al. (2023). Gas Discharge Source of Synchronous Flows of UV Radiation and Silver Sulphide Microstructures. *Physics and Chemistry of Solid State*, 24 (3), 417–421. <https://doi.org/10.15330/pccs.24.3.417-421>
24. Hrytsak, R., Shuaibov, O., Minya, O., Malinina, A., Shevera, I., Bilak, Y., Homoki, Z. (2024). Conditions for pulsed gas-discharge synthesis of thin tungsten oxide films from a plasma mixture of air with tungsten vapors. *Physics and Chemistry of Solid State*, 25 (4), 684–688. <https://doi.org/10.15330/pccs.25.4.684-688>

✉ **Yurii Bilak**, PhD, Associated Professor, Department of Systems Software, Uzhgorod National University, Uzhgorod, Ukraine, e-mail: yurii.bilak@uzhnu.edu.ua, ORCID: <https://orcid.org/0000-0001-5989-1643>

Fedir Saibert, PhD Student, Department of Systems Software, Uzhgorod National University, Uzhgorod, Ukraine, ORCID: <https://orcid.org/0009-0004-8081-4174>

Roman Buchuk, PhD, Department of Systems Software, Uzhgorod National University, Uzhgorod, Ukraine, ORCID: <https://orcid.org/0009-0000-4199-5583>

Mariana Rol, Senior Lecturer, Department of Systems Software, Uzhgorod National University, Uzhgorod, Ukraine, ORCID: <https://orcid.org/0000-0002-1120-8267>

✉ Corresponding author